Cross-vendor transfer and RF coil comparison of a high-resolution MP2RAGE protocol for brain imaging at 7T

Helms, Gunther ; Lätt, Jimmy; Olsson, Hampus

Published in:
Acta Scientiarum Lundensia

2020

Document Version:
Publisher's PDF, also known as Version of record

Volym ASL 2020-001

Citation: (Acta Scientiarum Lundensia)

Helms, G., Lätt, J., and Olsson, H., (2020). Cross-vendor transfer and RF coil comparison of a high-resolution MP2RAGE protocol for brain imaging at 7T, *Acta Scientiarum Lundensia*, Vol. 2020-001, pp. 2-12, ISSN 1651-5013

Acta Scientiarum Lundensia
(open access) Vol V2020-001 2020-05-11

Working paper in UHF MRI methods:

Cross-vendor transfer and RF coil comparison of a high-resolution MP2RAGE protocol for brain imaging at 7T

Gunther Helms[1], Jimmy Lätt[1,2], Hampus Olsson[1]

[1] *Lund University, Dept. of Clinical Sciences Lund, Medical Radiation Physics*
[2] *Skåne University Hospital (SUS) Lund, Dept. of Medical Imaging and Physiology*

Corresponding author: Gunther Helms,
Medical Radiation Physics, Barngatan 4, SE-22185 Lund, Sweden
E-mail: gunther.helms@med.lu.se

Abstract. An established MP2RAGE protocol for semi-quantitative structural brain MRI was transferred from one 7T MR scanner to that of another vendor featuring comparable hardware, but opposite polarity. On this system, the scan time could be reduced from 11 to 8 minutes, mainly by elliptical *k*-space sampling. Three configurations of radio-frequency (RF) transmission were compared (single channel with quadrature splitting, two and eight channels of fixed phase delays). Data processing for offline calculation MP2RAGE images is described in detail. The DICOM scaling of scanner B entails a loss of precision and accuracy and stronger artifacts in regions of low RF field, which can be improved by dielectric pads. For comparison and multi-site studies use of an identical scan protocol and identical RF hardware is recommended.

Keywords: quantitative MRI, structural imaging, T1 relaxation, brain, ultra-high field, signal scaling

1 Introduction

Structural Magnetic Resonance Imaging (MRI) is primarily based on local variations in the observed longitudinal relaxation time T_1, caused by the interaction of water molecules with proteins, lipid membranes and other macromolecular components (Fullerton et al., 1981, Rooney et al., 2007). MRI at ultra-high fields (UHF) (B_0>4T), MRI suffers from inhomogeneities of the radiofrequency (RF) fields. This is observed in three-dimensional (3D) MP-RAGE (magnetization-prepared rapid acquisition of gradient echoes) (Mugler III and Brookeman, 1990), especially if a volume RF coil is used for transmission and reception. The MP2RAGE technique (Marques et al., 2010) corrects for these effect by acquisition of a second RAGE train with predominant proton density weighting within the same cycle and using this second image to divide out local influence of flip angle, proton density and T_2^*. Because this enhances T_1-weighted contrast and corrects transmit and receive sensitivity, MP2RAGE has become the popular technique for structural MRI at UHF. In principle, MP2RAGE is a semi-quantitative technique that yields reproducible image intensities for follow-up of individuals or cohort comparisons. In addition, the underlying T_1 values can be retrieved by a look-up table.

Since semi-quantitative values by definition depend on the parameters of the MRI pulse sequence, a well-established MP2RAGE protocol was ported to a different 7T site and MR scanner. Primary objective of this traveling brain study was to assess the multi-site cross-vendor capability of the MP2RAGE technique. To this end, data management and calculation routines for MP2RAGE were established at the receiving site. Here, different configurations of the transmit RF coil were tested. Finally, the measurement time on the receiving system was systematically reduced using built in features of elliptical k-space sampling and a higher turbo factor.

2 Material and methods

2.1 MR equipment

The study was carried out on two different 7T MRI scanners at the Max-Planck-Institute for Human Cognitive and Brain Science, Leipzig, Germany (site A) and the National 7T facility, Lund University Bioimaging Center (LBIC) at Skåne University Hospital (SUS), Lund, Sweden (site B). Both were modified platforms of clinical 3T whole body MR systems of the first generation. Platform A was a Magnetom TRIO (Siemens Healthcare, Erlangen, Germany, software SynGo VA25); Platform B a Philips Achieva (Philips Healthcare, Best, The Netherlands, software release R5C). The 7T cryomagnets (Agilent Technologies, Oxford, UK) were operated at opposite polarities and at slightly different field strengths, corresponding to proton Larmor frequencies of 297.2 MHz on system A and of 298.0 MHz on system B. On both scanners, 16-rung birdcage resonators were used for transmission, and an array of 32 surface coil elements for reception (Nova Medical, Wilmington, MA). On system A, the transmit coil was driven via a single RF amplifier of 35kW peak power with fixed power splitting (Tx1). On system B (“Classic”), two ports were fed individually (Tx2), each by a solid-state RF amplifier of 4kW peak power. The phase difference of 120°, as optimized on site by staff of vendor B, was held constant (“fixed RF shims”). This coil can also be driven by equally splitting the output of one RF amplifier with 90° phase difference (“Quad” mode). A parallel transmit array by the same manufacturer, featuring eight parallel oriented strip-line T/R elements each driven with 45° phase differences by 1kW RF amplifiers (Tx8) was also tested on scanner B (“MTX”).

One healthy male subject (53 years) acted as a ‘traveling brain’ and was scanned two occasions on system A and three occasions on system B. On one occasion on system B, high permittivity dielectric pads containing calcium titanate in heavy water (provided by a material transfer agreement with Leiden University Medical Center, Leiden, The Netherlands) (Teeuwisse et al., 2012) were used to improve B_1^+ homogeneity (O'Brien et al., 2014). The study was performed over a time span of 14 months. Informed written consent as approved by the local Ethical Review Boards was obtained before each examination.

Table 1: Sequence parameters of the MP2RAGE protocol

A: Siemens 7T Magnetom	B: Philips 7T Achieva	value
Magn. Preparation	TFE pre-pulse	Non-sel.IR / invert
InvFlipAngle (deg)	Nominal angle (deg)	1800
TI1 (ms)	TI (ms)	900
TI2 (ms)	{TI + phase interval} (ms)	2750
{TI2 – TI1} (ms)	Phase interval (ms)	1850
TR (ms)	Cycle duration (ms)	5000
TE (ms)	TE (ms)	2.45
Bandwidth (Hz/pixel)	{1011 Hz / Water-fat-shift} (Hz/pixel)	250 / 310
{1011 Hz / Bandwidth} (pixel)	Water-fat-shift (pixel)	4.04 / 3.269
Echo spacing (ms)	TR (ms)	6.8
Flip angle 1 (deg)	Flip angle (deg)	5
Flip angle 2 (deg)	Flip angle 2nd pulse (deg)	3
Slices per slab	Encoding steps RL	256
-	Turbo direction	Z = Slice
Phase partial Fourier	Halfscan factor Y	0.75
Slice partial Fourier	Halfscan factor Z	1
GRAPPA acceleration factor	SENSE P reduction (AP)	2
Ref. lines PE	-	24 / -
Partial echo	Partial echo	off / no
Elliptical scanning	Elliptical k-space shutter	off / no

2.2 MP2RAGE protocol

The MP2RAGE protocol had been established at site A for quantitative structural imaging in cognitive neuroscience studies. A synopsis of values and vendor-specific terminology (marked by double-quotes ".") is given in Table 1.

The first volume was read out with 5° flip angle at TI1 = 900 ms after adiabatic inversion (1800° nominal flip angle); the second at TI2 = 2750 ms. Total TR of the cycle was 5000 ms. The readout trains of an equidistant spacing of 6.8 ms encoded 256 sagittal partitions (Turbo Factor) over a non-selective slab of 179 mm. Gradient echo-readout at TE = 2.45 ms with bandwidth of 250 Hz/pixel of 224 mm field-of-view (FoV) with an in-plane resolution of 0.7mm (matrix size 320x320). Acceleration was applied to the outer phase encoding loop using 75% partial Fourier encoding and "GRAPPA" (Griswold et al., 2002) (factor 2, 24 reference lines). This corresponds to 320*0.75/2 + 24/2 = 132 repetitions, that is, a total duration of 11 minutes. "Adaptive Combine" was used for phase-coherent combination of the 32 receive channels. Semi-quantitative MP2RAGE images ("UNI") and quantitative T_1 maps ("T1") were calculated inline and stored as 12 bit integer DICOMs along with the magnitude images "INV1" and "INV2" (Fig 1).

On scanner B, an MP2RAGE "scan" was set up replicating the timings, flip angles, and partial acquisition of scanner A. The peak B_1 amplitude was set to a value of 18 μT for Tx2 and Tx8, and 13 μT for Tx1, as this can be achieved in the vast majority of volunteers. Replicating the TE of system A entailed a 24% higher bandwidth of 310 Hz/pixel (303.8 Hz for Tx1). Since system B employs "SENSE" for parallel partial acquisition (Pruessmann et al., 1999), the low resolution reference scans have been acquired prior to the MP2RAGE scan. This entailed a scan time of 10 minutes. The 1 minute shortening corresponds to the 12 additional reference lines acquired on scanner A.

Scanner B offers further potential for accelerating the MP2RAGE scan, by employing an "elliptical *k*-space shutter" with "TFE" (Turbo Field Echo) acquisitions (proprietary functionality "3D Free Factor"). The "3D Free Factor" makes the encoding jump between nearby k_z lines, mostly in the periphery of k-space and less in the center, using the same "TurboFactor" of 256 as in linear encoding. This resulted in a scan time of 8:20 minutes. By virtue of

the "3D Free Factor", the "turbo direction" can be changed from "Y" (AP in sagittal orientation) to "Z" (RL). Finally, the "TurboFactor" was extended to 268, the maximum compatible with the chosen TI1, TI2 and TR, resulting in a scan time of 8:00 minutes. These four increasingly accelerated protocols were tested on the "classic" system B (Tx1, Tx2) and compared to the original MP2RAGE protocol of system A.

2.3 Data processing

Stacks of 2D DICOM images were converted into 3D NIfTI volumes, the most common format for imaging neuroscience studies (Li et al., 2016). Note, that the created sagittal volumes are consistent to the radiological right-left convention of transaxial or coronal images under 3D rotations (reversed slice numbering). Routines of the FMRIB software library FSL6 (fsl.fmrib.ox.ac.uk) were used for basic pre-processing (comprising manipulation of NIfTI structure, intensity scaling) and calculation of MP2RAGE images (see below), as well as co-registration, brain extraction, and histogram analysis. Shell scripts are available from the authors.

One scanner A, MP2RAGE volume was manually rotated to the anterior-commissure-posterior-commissure (ACPC) plane, shown in Fig. 3. This then served as individual template to co-register the other MP2RAGE volumes by a spatial rigid-body transform using the mutual information criterion. Thus, variation in subject position was accounted for and all MP2RAGE volumes were submitted to similar degrees of 3D linear interpolation. The $|S_{TI1}|$ and $|S_{TI2}|$ volumes were shadow-registered.

On system A, DICOM are saved four different series, which can be readily converted into NIfTI volumes. The 12 bit integer encoded "UNI" images were scaled to [–0.5, 0.5] by

$$MP2RAGE = (UNI - 2047)/4094 \in [-0.5, 0.5] \quad \text{Eq. (1)}$$

T1 values were encoded in units of millisecond and thus do not require scaling. A whole brain histogram is shown in Fig. 1.

On system B, the MP2RAGE images had to be calculated offline from the complex signals S_{TI1} and S_{TI2} as given in the original paper (Marques et al., 2010):

$$MP2RAGE = \frac{real\left(S_{TI1} \cdot S_{TI2}^{*}\right)}{|S_{TI1}|^2 + |S_{TI2}|^2} = \frac{real(S_{TI1})real(S_{TI2}) + imag(S_{TI1})imag(S_{TI2})}{real(S_{TI1})^2 + imag(S_{TI1})^2 + real(S_{TI2})^2 + imag(S_{TI2})^2}. \quad \text{Eq. (2)}$$

From the expanded formula on the right it becomes clear, that the result is not affected by swapping real and imaginary channels and/or their sign. It can also be expressed in terms of the image magnitude and phase:

$$MP2RAGE = \frac{|S_{TI1}|/|S_{TI2}|\cos\left(\phi_{TI1} - \phi_{TI2}\right)}{|S_{TI1}|^2/|S_{TI2}|^2 + 1}. \quad \text{Eq. (3)}$$

The appearance of $|S_{TI1}|/|S_{TI2}|$ in Eq. (3) indicates the semi-quantitative nature of MP2RAGE, because local B_1^- and B_1^+ are cancelled out. In addition, T_1 weighting is enhanced as the weighting by the inverse correlated proton density (Fullerton et al., 1981) and local T2* decay are removed by division (van de Moortele et al., 2009). Equation (3) also shows that S_{TI2}, which is read out from positive longitudinal magnetization M_z, serves as a reference for the local signal phase in the MP2RAGE acquisition. If S_{TI1} (after inversion recovery) is predominantly read out from positive M_z, the phase difference $\phi_{TI1} - \phi_{TI2}$ is close to zero and MP2RAGE is positive, but negative for negative M_z due to a phase difference of about π. The MP2RAGE approach thus enables signed inversion recovery imaging with gradient echo acquisition. The cosine projection of $\phi_{TI1} - \phi_{TI2}$ also reduces the phase noise, especially when S_{TI1} is close to 0.

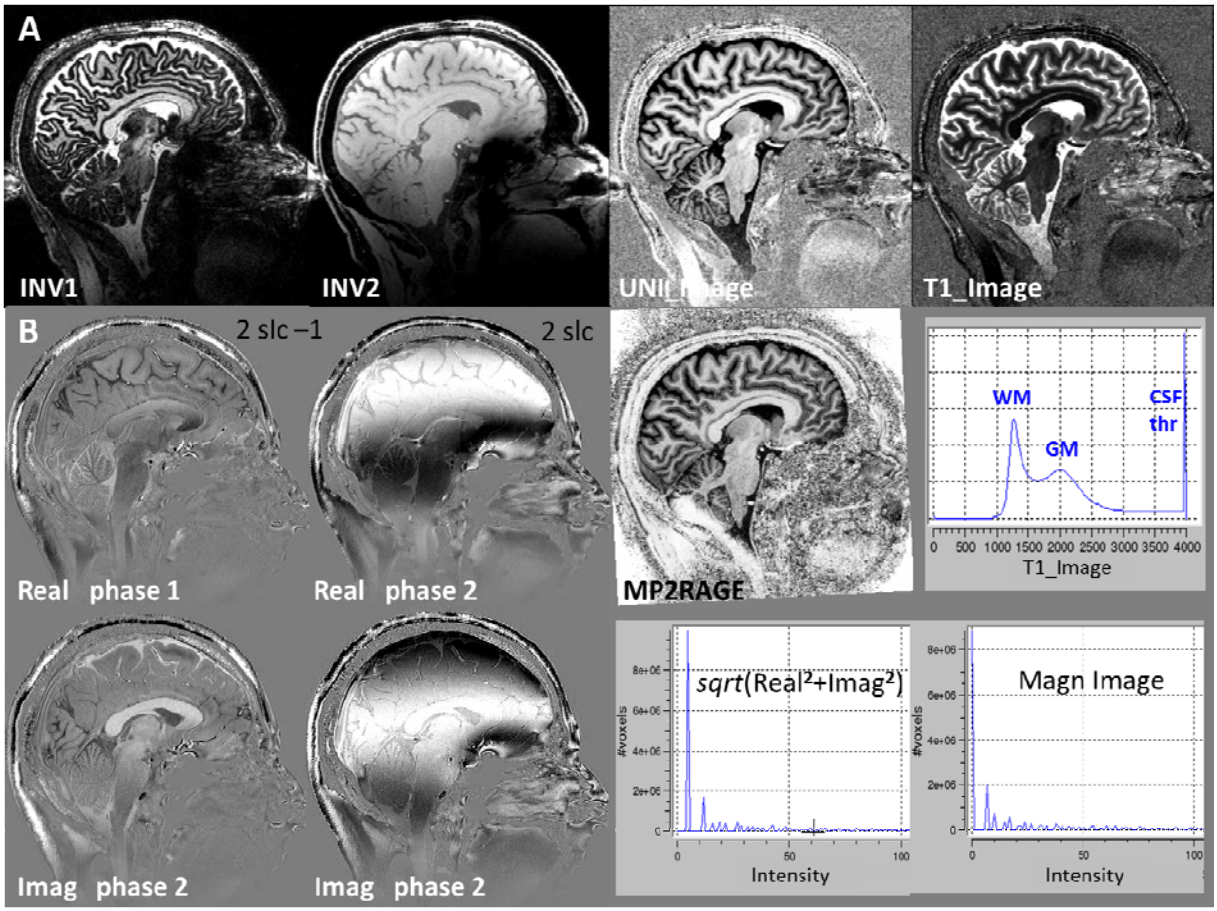

Fig 1 **DICOM output** -Top row: Images (magnitude) produced by scanner A, each representing a single volume. Estimated values in the T1_Image are displayed in the whole brain histogram below.
Lower left: Real and imaginary images of scanner B (displayed at the same contrast centered at zero. The bottom histograms demonstrate the zero shift in Real and Imag(inary) scaling, as well as the coarse digitization. Pixels with (0,0,0,0) thus appear with 0.5 in the MP2RAGE image (shown registered to the UNI image, 3rd panel of 2nd row).

Since *S* in Eq. (2) refers to the induced "physical" signal in consistent arbitrary units [a.u.], particular attention has to be given to consistent signal scaling. To perform the complex multiplication, additional volumes of datatype "R"(eal) and "I"(maginary) were stored as DICOMs (Fig. 1), displayed as floating values with individual scaling parameter for each individual volume as documented in the DICOM tags (0028,1052, Rescale Intercept) and (0028, 1053, Rescale Slope). Identical rescaling (0028, 1054, Rescale Type=normalized) is used in the two "phases" and for the real and imaginary signals of the same "scan". By calculating the signal magnitude from the real and imaginary DICOMs and comparison to magnitude DICOM, one can see that the rescaling shifts the zero to value –Rescale Slope/2 (see histograms at bottom of Fig. 1). Pixels containing zeros only (mainly at some distance from head) are thus assigned MP2RAGE = 0.5 (Fig. 1). In addition, the actual dynamic range of intensities covered typically only 256 (of 4096 available) values, entailing a considerable loss of precision.

2.4 Data formats, export and conversion to NIfTI from system B

Immediate reconstruction of multiple datatypes on system B (as specified under 2.3) yields datasets of five dimensions (3 spatial + "phases" + datatype), which may cause conversion problems to 4D NIfTI. For freeware dicom to NIfTI converters, it is therefore recommended to reconstruct "R"eal and "I"maginary DICOMs in two

individual “delayed recon”(struction) processes, each of which will create a dataset of 4 dimensions (3 spatial + “phases”) compatible to the NIfTI format. Such 4D data structures further facilitate the access and offline calculation by NIfTI-based software packages like FSL.

2.4.1. Dicom export to “7T archive”

DICOM data from 7T may be exported to a dedicated “7T Archive” server, which grants access to anonymized download outside SUS via a one-time password by registered extra-mural users of the National 7T facility.
The 6-digit numbering of the DICOM filename alternates between the two “phases”, that is, TI1 and TI2. If both “Real” and “Imaginary” images are created, the Imaginary volumes are appended (outer loop=data type). When individual DICOMs are processed, the MP2RAGE of number slc of 256 sagittal slices is calculated from the DICOM images 2slc–1, 2slc, 2slc+511, and 2slc+512.

In 5D MP2RAGE datasets, the surplus datatype dimension is sometimes stacked along the *z*-direction. In this case, “R”eal and “I”maginary volumes have to be extracted using the “`fslroi`” command with the appropriate matrix sizes for further processing in FSL. As noted above such manipulations are avoided, when subseries of “R” and “I” images are created by individual steps of “Delayed Recon”.

It is also important to note, that when stacking DICOM images into volumes by ascending numbers, that the numbering of sagittal 2D images will result in swapping the R(ight)L(eft) dimension (into LR neuroscience convention) when compared to standard volumes created from transaxial images. For example, this applies when using MRIcro (Rorden) to manually create volumes in the legacy Analyze format. A NIfTI volume in the standard ‘radiological’ transaxial space is created by reordering the spatial dimensions using the fsl command line

```
fslswapdim <sag-volume> z –x y <tra-volume>
```

2.4.2. NII conversion via local image processing pipeline

Dicom images were transferred to a local server at the Department of Medical Imaging and Physiology (BoF), pseudonymized, and converted to NIfTI volumes for further processing using the legacy dcm2nii DICOM to NIfTI converter of MRIcron (Rorden). These contain the “displayed values”, that is 32 bit float values that have been “re-scaled” from the stored 12 bit integers (see above). Different datatypes are stored in separate files. NIfTIs containing real, imaginary or phase data are marked by suffixes “R_FFE_R_FFE”, “I_FFE_I_FFE”, or “PHASE_FFE_P_FFE”, respectively.

A second conversion (“NIIscaled”) of DICOMs from scanner B to physical signal intensities (“Floating point values”) was performed using an in-house modification of the Matlab routines of (Li et al., 2016). After applying pertinent parameters in the private tags (2005,100D, MR Scale Intercept) and (2005,100E, MR Scale Slope) (Chenevert et al., 2014) , the values were divided by 1000 to obtain values similar to those from other systems and phase values in radians. The spatial dimensions of sagittal and coronal volumes are reordered to standard transaxial orientation, but otherwise, the 4D structure of datasets is maintained in the NIfTI files. The DICOM-encoded values of maps calculated in-line by scanner B are preserved. The recovery of the physical MR signal, however, did not eliminate the zero offset by half a digitization step from the displayed values (see above). Thus, both “Displayed values” and “Floating point values” resulted in identical MR2RAGE images.

2.4.3. Export in proprietary par/rec format

The MP2RAGE data can also be exported to a physical drive in the proprietary “par/rec” format of vendor B, maintaining the 5D data structure. “par/rec” files can be read directly into MatLab by a script provided by the vendor.

For use with third party conversion programs, “sorted” conversion is recommended. Legacy Analyze volumes created from par/rec data using MRIcro will be consistent with the radiological RL convention. Standard transaxial NIfTI volumes are thus created by (note sign change in dim1) compared to 2.4.2

```
fslswapdim <sag-volume> –z –x y <tra-volume>
```

3 Results

The inversion recovery at TI1 yielded the gray matter (GM) signal close to zero, while the faster T_1 relaxation of white matter (WM) lead to higher signal. The unusual contrast of the magnitude images (Fig. 1) is due to the negative M_z of slowly relaxing cerebro-spinal fluid (CSF). The contrast of the second image is dominated by the proton density. Both intensities are modulated by the spatial inhomogeneity of the radio-frequency fields of the transmit coil (B_1^+) and receive coils (B_1^-) (van de Moortele et al., 2009).

Because of the small FoV, the tip of the nose usually extends beyond the border of the FoV. With GRAPPA, the nose is folded over into the posterior FoV. The proprietary SENSE algorithm is able to suppress small fold-ins, but will eventually show artifacts in the center (factor 2). With SENSE, the FoV should be rotated in-plane to cover the whole nose.

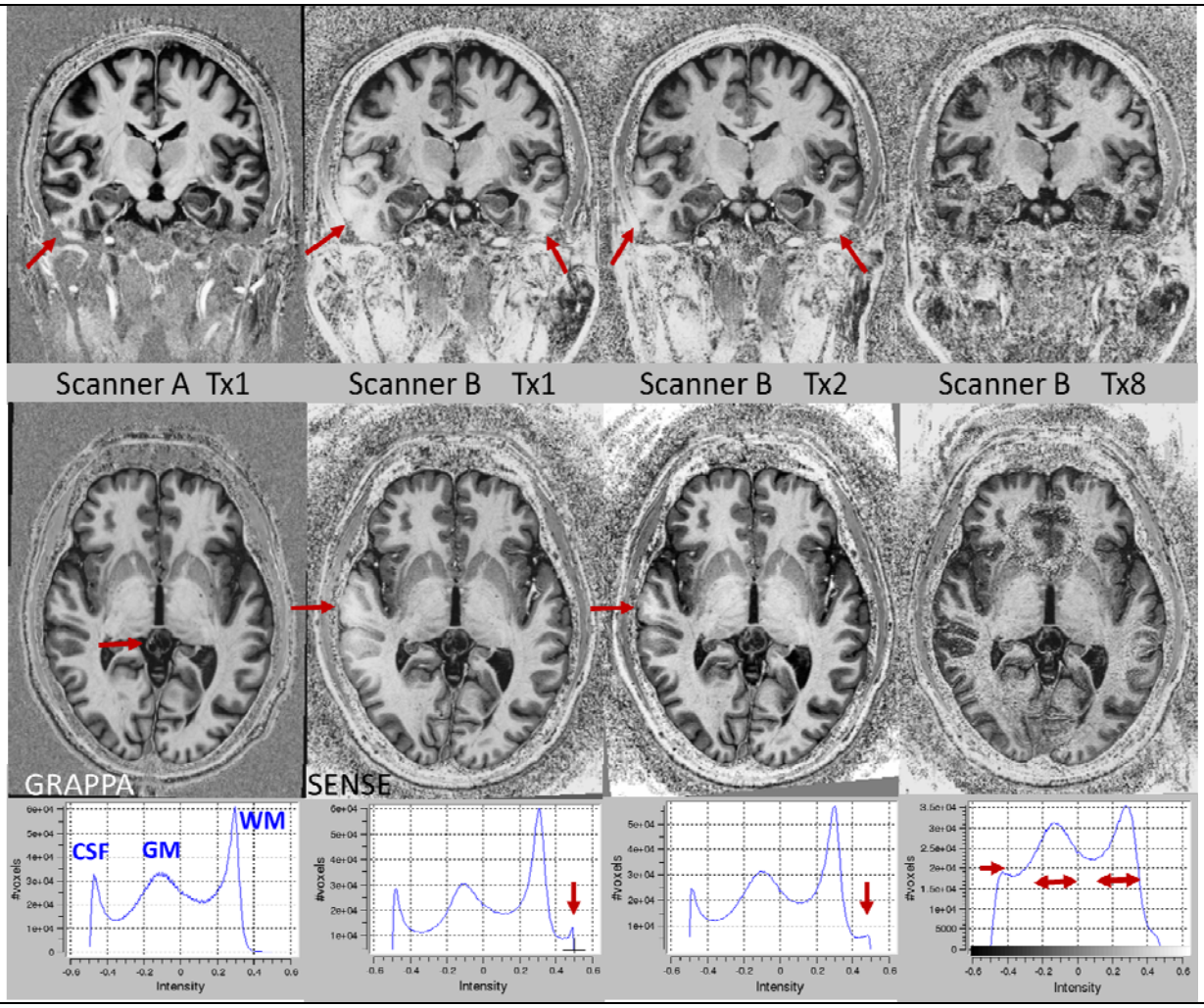

Fig 2 MP2RAGE obtained on scanner A (left) and with different coils on scanner B
Top row: Coronal view depicting artifacts in the inferior frontal lobes. Middle row: Transversal ACPC plane depicting cortical and deep brain structures. Bottom row: Whole brain histograms (201 bins) showing the frequency of artefacts and malfunctioning MTX coil. The features highlighted by arrows are described in the text.

3.1 Benchmarking of RF coils on system A and system B

On system A, the pixels in air showed little structured noise (compliant subject), due to the GRAPPA reference lines and reconstruction being integrated in *k*-space (Griswold et al., 2002). On system B, the SENSE algorithm (Pruessmann et al., 1999) created structured noise adjacent to the head due to spatial interpolation and filtering. This consequently shows in the MP2RAGE images.

The contrast of MP2RAGE in the cerebrum was very similar, as seen in Fig. 2. However, scanner B yielded lower signal-to-noise ratio (SNR) than scanner A due to a higher bandwidth and lack of 12 low-frequency *k*-space lines. Nevertheless, narrow structures like the wall of the pineal cyst (arrow) were less well delineated on scanner A. System A showed considerably less in-flow-related hyperintensities in the ascending arteries than system B (transaxial slices in Fig. 2) and provided higher signal intensities in the cerebellum and more inferior regions (Fig. 3). This observation is in line with the slightly larger axial dimension of the transmit coil of system A. This problem may have been exacerbated by SENSE since this method maps the sensitivities onto the B_1^- field of the transmit coil, notwithstanding the readout in the B_0 direction.

System B showed larger areas of hyperintense artifacts in cerebellum (Fig. 4) and in the right temporal cortex (arrow) than scanner A, which are also identified in the whole brain histograms (arrow). The opposed laterality in the cerebellum shown that arise from regions of low B_1^+ and B_1^- of the transmit coil. Thus, they are smaller when the birdcage transmit coil was driven by two channels and almost disappeared with the Tx8 stripline elements of the MTX system (right). Though the MTX system provided better coverage of the cerebellum and inferior head, the much reduced SNR (showing as broadened peaks in the histogram) is hitherto unexplained as SNR should be determined by the 32 receive elements. The bands of noise artifacts in the MP2RAGE images may indicate further instabilities in the transmit hardware.

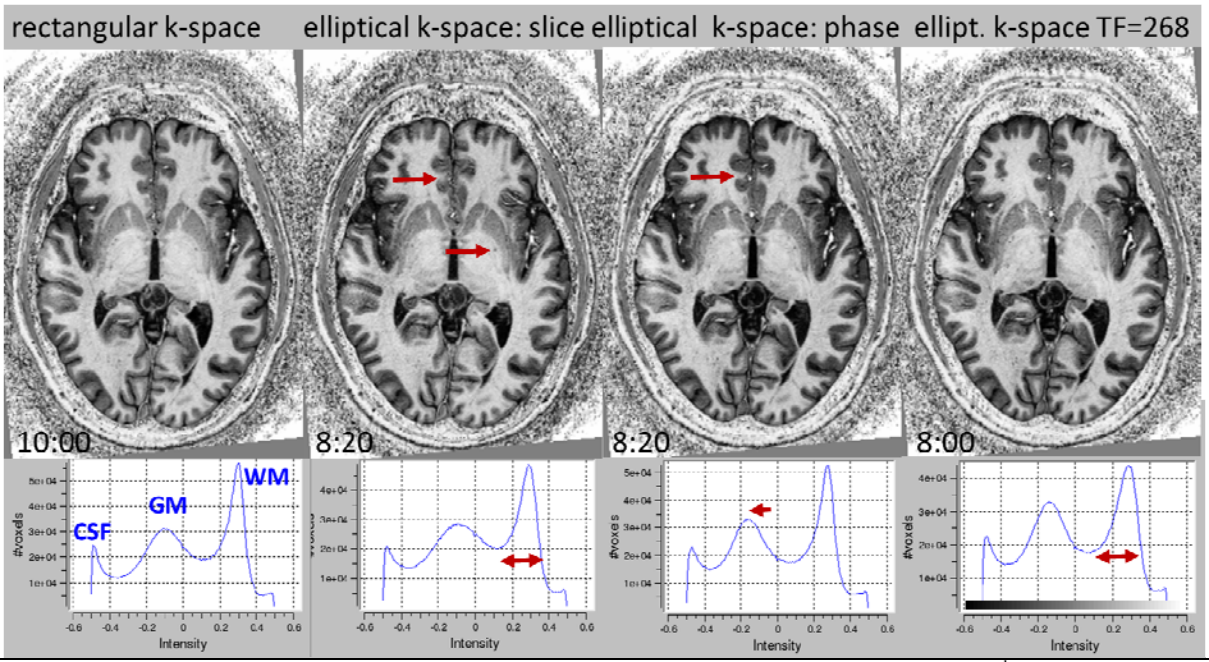

Fig 3 Top row: MP2RAGE obtained on scanner A (left), with the protocol transferred to scanner B (2nd left), with elliptical k-space coverage (center) plus turbo direction Y (2nd right) and with the maximum turbo factor of 268 (right)
Bottom row: Whole brain histograms (201 bins) revealing subtle changes in the intensity distribution. Features highlighted by arrows are described in the text.

3.2 Acceleration of MP2RAGE on system B

The application of elliptical k-space sampling ("3D Free Factor") did hardly change the MP2RAGE intensities, as seen by comparing the histograms in Fig. 3. However, the main modes of WM, GM, and CSF appeared slightly broadened, which may be tentatively explained by redistributing the k-space lines along the read-out affecting the point-spread function. Thus, small features of high contrast like perivascular spaces in WM appeared somewhat smoothed, as demonstrated by a vessel in the globus pallidus (arrow). In addition, artefacts were seen in the anterior cingulate cortex next to the anterior cerebral artery. These disappeared after changing the "turbo direction" from "Z" to "Y" (arrow). Serendipitously, this also yielded narrower modes in the histogram and lowered the GM intensity (arrow) resulting in a better GM-WM contrast. Finally, increasing the turbo factor to its maximum did not change the appearance of the MP2RAGE images, but subtle contrast changes (like slightly reduced WM intensity) can be inferred from the broadened peaks in the histogram (arrow). The same behaviour was observed when operating the coil with quadrature power splitting (Tx1) (not shown).

3.3 Repeatability and reproducibility

Figure 3 shows identical coronal views of five MP2RAGE experiments. On system B, the 8 minute protocol was performed on the Tx2 coil, and the 11 minute protocol on scanner A. This coronal view shows the extense of the hyperintense artefacts in the left cerebellum on scanner A, which hardly extended into the inferior temporal lobes as seen on scanner B. The opposed laterality indicates that these are related to the polarity of the magnets and thus the birdcage transmit coils. Although these hyperintensities destroyed the contrast of the cortical boundary of the inferior temporal lobes, they were quite reproducible. The high-permittivity dielectric pads ameliorated the problem in the temporal lobe, which nevertheless persisted in the most inferior parts and was "shifted" towards the other cerebellar hemisphere (not shown). Note that the pads are visible on MP2RAGE and their positioning is expected to negatively affect reproducibility.

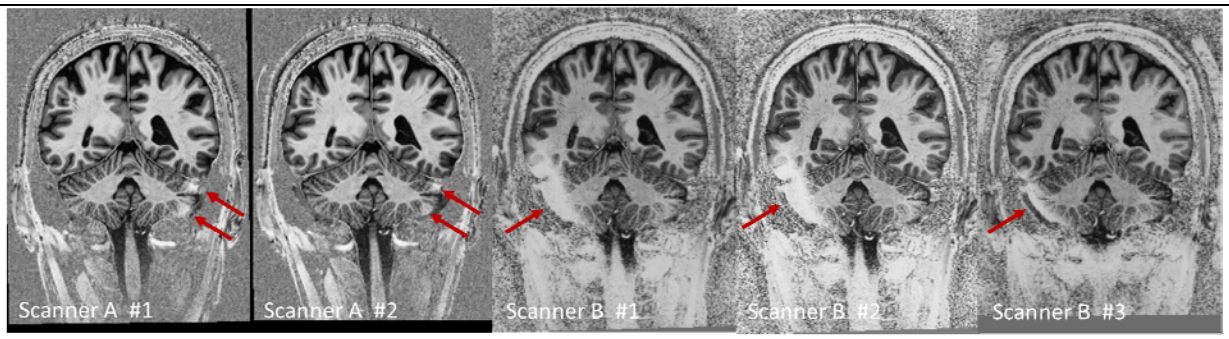

Fig 4 Coronal views of the MP2RAGE images acquired at 5 repeated sessions.

4. Discussion and Conclusion

An MP2RAGE protocol was transferred from a 7T Siemens MR scanner (on which this technique had originally been established (Marques et al., 2010)) to a 7T Philips MR scanner equipped with hardware components of near-identical specifications. Equal intensity differences between GM and WM on one hand and GM and CSF on the other render this protocol suitable for determination of the cortical boundaries. The intensity in GM value depends strongly on the chosen first TI. Note that GM was not adjusted to less than zero to avoid the dynamic M_z changing sign near zero k-space, which may lead to image artifacts.

This major contrast in brain could be reproduced on both systems, but scanner B suffered from lower SNR and much larger regions were affected by artifacts. These were much reduced using the eight-channel transmit coil ("MTX"), which also had a better brain coverage. It must be pointed out that the MTX-related artifacts were due to intermittent instabilities and thus not representative. These were linked to the performance of RF transmit coil by their specific laterality. A multi-vendor comparison of MP2RAGE is thus not possible in the affected regions, even when using RF equipment from the same vendor. Such artifacts will hamper further processing by voxel-based morphology (VBM) (Ashburner and Friston, 2000) or cortical segmentation. These findings confirm that identical RF hardware is required for quantitative cohort studies. MP2RAGE may thus improve, but not totally overcome the difficulties experienced with structural MP-RAGE (Focke et al., 2011).

The larger artifacts observed with the Tx2 operation are somewhat unexpected, because in theory this should allow for a better adaption to individual anatomy. Tx2 gave better results than the "naïve" 50% quadrature power splitting on the same scanner. Technical details of the dedicated power splitter for Tx1 operation are proprietary of Nova Medical.

The simple calculation of MP2RAGE images was scripted in FSL, to be implemented into the local data pipeline. However, this required careful data management and control of the rather complicated intensity scaling. UNI images (system A) were calculated in-line with floating point precision. Storage of complex signal as 12 bit DICOMs on system B, however, imposes loss of some precision and accuracy in the calculated semi-quantitative MP2RAGE images. This may be ameliorated by using magnitude and phase images (Eq. 3). DICOM images of real and imaginary signals were created by successive "delayed reconstructions" to make them compatible with the local automated data processing pipeline. Acquisition of multi-echo MP2RAGE is possible on system B (Caan et al., 2019), but will eventually result in six dimensional datasets.

More complicated processing should be done in MatLab. Underlying T_1 values are determined from MP2RAGE images by a look-up table, which could not be implemented into FSL. Pertinent MatLab code can be obtained from W. Van der Zwaag, Spinoza Center, Amsterdam. The T_1 maps obtained on scanner A were in agreement to those obtained by single-slice Look-Locher (Rooney et al., 2007) and the 3D dual flip angle (DFA) method (Olsson et al., 2020). The MP2RAGE scan was of higher resolution and did not require additional B_1^+ mapping.

Partial parallel acquisition by SENSE on system B allowed for faster acquisition than GRAPPA on system A at the cost of SNR and motion artifacts. Further acceleration to 8:20 minutes without apparent loss of quality was achieved using the FreeFactor feature of system B. With subtle variation across WM and GM, tentatively due to MT effects immediately after inversion (Rioux et al., 2016), the scan time for MP2RAGE with 0.7mm isotropic resolution was thus reduced from 11 minutes to 8 minutes.

.

Acknowledgements

G.H. was funded by Swedish Research Council (NT 2014-6193). The reference MP2RAGE protocol was kindly provided by Dr. Robert Trampel, Max-Planck-Institute for Human Cognition and Brain Sciences, Leipzig, Germany. Lund University Bioimaging Center (LBIC) is acknowledged for experimental resources (equipment grant VR RFI 829-2010-5928).

References

ASHBURNER, J. & FRISTON, K. J. 2000. Voxel-Based Morphometry—The Methods. *NeuroImage,* 11**,** 805–821.

CAAN, M., BAZIN, P., MARQUES, J., DE HOLLANDER, G., DUMOULIN, S. & VAN DER ZWAAG, W. 2019. MP2RAGEME: T1 , T2 * , and QSM mapping in one sequence at 7 Tesla. *Hum Brain Mapp,* 40**,** 1786-1798.

CHENEVERT, T., MALYARENKO, D., NEWITT, D., LI, X., JAYATILAKE, M., TUDORICA, A., FEDOROV, A., KIKINIS, R., LIU, T., MUZI, M., OBORSKI, M., LAYMON, C., LI, X., THOMAS, Y., JAYASHREE, K., MOUNTZ, J., KINAHAN, P., RUBIN, D., FENNESSY, F., HUANG, W., HYLTON, N. & ROSS, B. 2014. Errors in Quantitative Image Analysis due to Platform-Dependent Image Scaling. *Transl Oncol,* 7**,** 65-71 eCollection.

FOCKE, N. K., HELMS, G., KASPAR, S., DIEDERICH, C., TOTH, V., DECHENT, P., MOHR, A. & PAULUS, W. 2011. Multi-site voxel-based morphometry - Not quite there yet. *Neuroimage,* 56**,** 1164-1170.

FULLERTON, G. D., POTTER, J. L. & DORNBLUTH, N. C. 1981. NMR relaxation of protons in tissues and other macromolecular water solutions. *Magn Res Imaging,* 1**,** 209-228.

GRISWOLD, M. A., JAKOB, P. M., HEIDEMANN, R. M., NITTKA, M., JELLUS, V., WANG, J., KIEFER, B. & HAASE, A. 2002. Generalized autocalibrating partially parallel acquisitions (GRAPPA). *Magn Res Med,* 47**,** 1202–1210.

LI, X., MORGAN, P. S., ASHBURNER, J., SMITH, J. & RORDEN, C. 2016. The first step for neuroimaging data analysis: DICOM toNIfTI conversion. *J Neurosc Methods,* 264**,** 47–56.

MARQUES, J. P., KOBER, T., KRUEGER, G., VAN DER ZWAAG, W., VAN DE MOORTELE, P.-F. & GRUETTER, R. 2010. MP2RAGE, a self bias-field corrected sequence for improved segmentation and T_1-mapping at high field. *NeuroImage,* 49**,** 1271-1281.

MUGLER III, J. & BROOKEMAN, J. 1990. Three-dimensional magnetization-prepared rapid gradient-echo imaging (3D MP-RAGE). *Magn Reson Med,* 15**,** 152-157.

O'BRIEN, K. R., MAGILL, A. W., DELACOSTE, J., MARQUES, J. P., KOBER, T., FAUTZ, H.-P., LAZEYRAS, F. & KRUEGER, G. 2014. Dielectric pads and low-B_1^+ adiabatic pulses: Complementary techniques to optimize structural T1w whole-brain MP2RAGE scans at 7 Tesla. *J Magn Reson Imaging,* 40**,** 804-812.

OLSSON, H., ANDERSEN, M., LÄTT, J., WIRESTAM, R. & HELMS, G. 2020. Reducing bias in dual flip angle T_1-mapping in human brain at 7T. *Magn Reson Med,* (submitted).

PRUESSMANN, K. P., WEIGER, M., SCHEIDEGGER, M. B. & BOESIGER, P. 1999. SENSE: Sensitivity encoding for fast MRI. *Magn Reson Med,* 42**,** 952–962.

RIOUX, J. A., LEVESQUE, I. R. & RUTT, B. K. 2016. Biexponential longitudinal relaxation in white matter: Characterization and impact on T_1 mapping with IR-FSE and MP2RAGE. *Magn Reson Med,* 75**,** 2265-2277.

ROONEY, W., JOHNSON, G., LI, X., COHEN, E., KIM, S., UGURBIL, K. & SPRINGER, C. J. 2007. Magnetic field and tissue dependencies of human brain longitudinal ^1H_2O relaxation *in vivo*. *Magn Reson Med,* 57**,** 308-318.

RORDEN, C. *dcm2nii DICOM to NIfTI conversion* [Online]. Available: people.cas.sc.edu/rorden/mricron/dcm2nii.html [Accessed].

RORDEN, C. *MRIcro web pages* [Online]. Available: people.cas.sc.edu/rorden/mricro/index.html [Accessed].

TEEUWISSE, W., BRINK, W. & WEBB, A. 2012. A quantitative assessment of the effects of high permittivity pads in 7 Tesla MRI of the brain. *Magn Reson Med,* 67**,** 1285-1293.

VAN DE MOORTELE, P.-F., AUERBACH, E. J., OLMAN, C., YACOUB, E., UGURBIL, K. & MOELLER, S. 2009. T_1 weighted brain images at 7 Tesla unbiased for proton density, T_2^* contrast and RF coil receive B1 sensitivity with simultaneous vessel visualization. *NeuroImage,* 46**,** 432-446.